Assessment of Microbiologically Influenced Corrosion Potential in the *International Space Station* Internal Active Thermal Control System Heat Exchanger Materials: A 6-Mo Study

Monsi C. Roman
NASA Marshall Space Flight Center, Huntsville, Alabama, USA

Patrick Macuch and Thomas McKrell
Altran Corporation, Boston, Massachusetts, USA

Ockert J. Van Der Schijff
CorrConsult, Ashland, Massachusetts, USA

Ralph Mitchell
Harvard University, Cambridge, Massachusetts, USA

ABSTRACT

The fluid in the Internal Active Thermal Control System (IATCS) of the *International Space Station* (*ISS*) is water based. The fluid in the *ISS* Laboratory Module and Node 1 initially contained a mix of water, phosphate (corrosion control), borate (pH buffer), and silver sulfate (Ag_2SO_4) (microbial control) at a pH of 9.5±0.5. Over time, the chemistry of the fluid changed. Fluid changes included a pH drop from 9.5 to 8.3 due to diffusion of carbon dioxide (CO_2) through Teflon® (DuPont) hoses, increases in dissolved nickel (Ni) levels, deposition of silver (Ag) to metal surfaces, and precipitation of the phosphate (PO_4) as nickel phosphate ($NiPO_4$). The drop in pH and unavailability of a antimicrobial has provided an environment conducive to microbial growth. Microbial levels in the fluid have increased from <10 colony-forming units (CFUs)/100 mL to 10^6 CFUs/100 mL.

The heat exchangers in the IATCS loops are considered the weakest point in the loop because of the material thickness (≈7 mil). It is made of a Ni-based braze filler/CRES 347. Results of a preliminary test performed at Hamilton Sundstrand indicated the possibility of pitting on this material at locations where Ag deposits were found. Later, tests have confirmed that chemical corrosion of the materials is a concern for this system. Accumulation of micro-organisms on surfaces (biofilm) can also result in material degradation and can amplify the damage caused by the chemical corrosion, known as microbiologically influenced corrosion (MIC).

This paper will discuss the results of a 6-mo test performed to characterize and quantify the damage from microbial accumulation on the surface of the *ISS* IATCS heat exchanger materials. The test was designed to quantify the damage to the materials under worst-case conditions with and without micro-organisms present at pH 8.3 and 9.5.

INTRODUCTION

The IATCS on the *ISS* is a closed-loop system that provides a constant temperature to equipment, payloads, and avionics. The IATCS loop is composed of two loops—the moderate-temperature loop (MTL) with 200 L of fluid at a supply temperature of 16.1 to 18.3 °C and the low-temperature loop (LTL) with 63 L of fluid at a supply temperature of 3.3 to 6.1 °C. The loops were designed to operate independently or in a single-loop mode while maintaining their respective temperature range. The fluid in the IATCS loops is water based, containing phosphate (corrosion control), borate (pH buffer), and Ag_2SO_4 (microbial control). The *ISS* specifications require the pH of the solution to be maintained at 9.5±0.5.

Changes in the chemistry of the IATCS fluid have been documented since the loops in Node 1—the first United States *ISS* element—were charged and operated. These changes include the following:

- The concentration of antimicrobial Ag dropped quickly due to deposition on the loop metals.

- The pH dropped from 9.5 to 8.4 due to diffusion of CO_2 through Teflon® hoses.
- Total organic carbon (TOC), total inorganic carbon (TIC), and dissolved Ni have increased in concentration.
- The initial concentration of ammonia increased.
- Concentrations of heterotrophic bacteria in the fluid increased from <10 CFUs/100 mL to 10^6 CFUs/100 mL since the first samples were returned to the ground for microbial analysis in 1999.

Uncontrolled microbiological growth in the IATCS can deteriorate the performance of the system and potentially impact human health if opportunistic pathogens become established in the system. Micro-organisms are capable of degrading the coolant chemistry and initiation/acceleration of hardware corrosion. In addition, attachment to surfaces and subsequent biofouling of filters, tubing, and pumps could decrease flow rates, reduce heat transfer, and enhance mineral scale formation.

MIC describes a complex set of interactions between a corroding metal or alloy, a consortium of micro-organisms, and the surrounding environment. Metal corrosion, in general, is essentially an electrochemical process whereby metals are oxidized and released from the metal surface at an anodic site, while at the same time the electrons resulting from metal oxidation reduce a chemical species that is in contact with the metal surface at a cathodic site. Metal corrosion occurs in the absence of micro-organisms; however, when either the anodic or cathodic reaction is initiated or accelerated by microbiological activities, the corrosion process is referred to as MIC. [1]

There is no established correlation between the numbers and types of micro-organisms in the fluid and the microbial population living in a biofilm. Furthermore, there is no established correlation between the numbers and types of micro-organisms in the fluid or in a biofilm and the likelihood of MIC. [2]

At this time, there are no standard methods for MIC testing. The American Society for Testing and Materials began the development of standards on MIC testing in 1991. It is expected that, in the near future, test standards will be available. For the microbiologically influenced corrosion accelerated test (MAT), the testing protocol was prepared after an extensive review of published methodology and the understanding of the hardware operating parameters. Appropriate controls to distinguish between biotic and abiotic corrosion effects, as well as to compensate for artifacts associated with some analytical techniques, were incorporated into the test. A combination of electrochemical, metallurgical, surface analytical, and microbiological techniques were used in this test to assess the effect of MIC on the test coupons.

The objective of this study was to assess and quantify the damage from microbial accumulation on the surface of the *ISS* IATCS heat exchanger materials at pH 8.3 and 9.5. The heat exchangers are considered the weakest point of the system because the thickness of the material between the water (IATCS) and the external fluid (ammonia) is 7 mil thick. A failure of the heat exchanger could have catastrophic results to the *ISS*. The MAT described in this paper was designed to simulate the operating parameters of the *ISS* IATCS and provide an assessment of in situ worst-case material corrosion rates over a 6-mo timeframe.

METHOD

The MAT system was designed to expose the test coupons to a laminar flow of IATCS solution in the presence and absence (control) of a microbial consortium composed of isolates from the on-orbit loops. Sterilized Pyrex kettles (bioreactors) containing 2 L of sterile, filtered (0.2-µ cellulose acetate membrane) IATCS solution were housed in microbiological incubator cabinets set at 27±1 °C. IATCS solutions were maintained at pH 8.3 or 9.4 by the addition of a CO_2 gas mixture. The IATCS solution was pumped through each test loop at a linear velocity of 0.33 ft/s using peristaltic pumps. The laminar flow and velocity simulated the *ISS* heat exchanger operating conditions on orbit. The fluid recirculated on a continuous basis using size 17 Norprene® food grade tubing (Cole Parmer) and was continuously mixed using a magnetic stirrer. A triplicate series of flow cells—for 30-, 90-, and 180-d sample exposure testing—received IATCS solution from a single bioreactor and pump head. The MAT bioreactors were vented through sterile air filters with silicone tubing connected to a water lock system to prevent backflow addition of air and alleviate any pressure from the addition of CO_2 and/or microbial activity.

COUPON LOADING INTO FLOW CELLS - Preconditioned braze material with nickel filler-2 (BNi-2) and BNi-3 coupons (coupons previously exposed to fluid with Ag) were fixed onto high-density polyethylene plastic backing plates (flow cell middle plate) with food-safe silicone adhesive (Dow Corning, RTV 732). The sample coupons were sufficiently separated (distance between samples = 50 × flow channel height) to minimize turbulence. The coupon backing plate allowed for removal of the coupons from the flow cell without damaging or contaminating them with debris from the silicone adhesive after MAT exposure. After the adhesive had cured, a subset of the coupons was measured for their height (thickness) above the flow cell backing plates. This was done to determine the average sample height and determine the peristaltic pump rate that would be required to achieve an average flow rate of 0.33 ft/s of IATCS fluid across the surfaces of the coupon samples when in the MAT system flow cells.

Prior to the start of the test, the flow cells were assembled, filled with 70% isopropyl alcohol (IPA), and allowed to stand for 5 min for disinfection. After disinfection, the flow cells were flushed once with 200 mL of sterile, filtered IATCS solution ($\approx$10 times the volume of the flow cell) at the appropriate pH to remove the IPA. The flow cells were then loaded into the MAT system and the flow of IATCS solution started.

MAT SYSTEM INOCULATION - The MAT system bioreactors A1–A4 were inoculated with the strains isolated from the *ISS* and with the sulfate-reducing bacterium (SRB) *Desulfovibrio desulfuricans*. Tables 1 and 2 contain the list of the bioreactor labels, pH of the fluid, and materials. Table 3 contains a list of the organisms that were used. Pure cultures of bacterial strains isolated from on-orbit IATCS solution were grown aerobically on R2A medium for 5 d at 30 °C for test inoculum preparation. Cells of the pure bacterial strains were harvested from R2A medium and suspended to a concentration of $\approx 1 \times 10^9$ cells/mL (McFarland Standard, Biomerieux) in 5 mL of sterile, filtered IATCS solution. The SRB was grown at 30 °C for 7 d anaerobically in a Forma Model 1025 anaerobic chamber on Baar's medium [3], and also prepared for inoculation to the MAT system. The cell suspensions were first washed twice in IATCS solution by centrifuging the cells at 3500 X G and resuspending in 5 mL of sterile IATCS solution. The single strain cell suspensions were then combined to prepare an inoculum of all strains for the MATs. Fifteen milliliters of the suspension was used to inoculate each bioreactor to a final concentration of $\approx 10^8$ CFUs/100 mL of each strain in the exposure MATs. Control bioreactors were not inoculated. All of the bacterial species were inoculated within 1.3 logs (range zero to 1.3) of the desired starting concentration of 1×10^6 cells/mL.

TEST MONITORING AND CONTROL

pH Monitoring and Control - The IATCS solution was buffered with borate to a pH of 9.5. The pH of the IATCS solutions in the MAT bioreactors was maintained at either 8.3 or 9.4 (± 0.2). The pH of the IATCS solution in the bioreactors was maintained at 8.3 by sparging a

Table 1. MAT Test Parameters of Inoculated Bioreators

Bioreactor Identification	Bioreactor IATCS pH	Sample Coupon Material	Sample Test Day	Flow Cell No.	Coupon Sample No.	Flow Cell Sample Position
A1	8.3	BNi-3	30	1	320	1
					321	2
					322	3
					323	4
			90	2	324	1
					325	2
					326	3
					327	4
			180	3	328	1
					329	2
					330	3
					331	4
A2	8.3	BNi-2	30	13	200	1
					201	2
					202	3
					205	4
			90	14	206	1
					207	2
					210	3
					211	4
			180	15	212	1
					215	2
					216	3
					217	4
A3	9.4	BNi-3	30	7	352	1
					353	2
					354	3
					355	4
			90	8	356	1
					357	2
					358	3
					377	4
			180	9	360	1
					361	2
					362	3
					363	4
A4	9.4	BNi-2	30	19	243	1
					222	2
					240	3
					241	4
			90	20	266	1
					245	2
					246	3
					267	4
			180	21	265	1
					249	2
					250	3
					264	4

Table 2. MAT Test Parameters of Uninoculated Bioreators

Bioreactor Identification	Bioreactor IATCS pH	Sample Coupon Material	Sample Test Day	Flow Cell No.	Coupon Sample No.	Flow Cell Sample Position
B5	8.3	BNi-3	30	4	332	1
					333	2
					334	3
					335	4
			90	5	336	1
					337	2
					338	3
					376	4
			180	6	340	1
					345	2
					350	3
					351	4
B6	8.3	BNi-2	30	16	220	1
					221	2
					223	3
					224	4
			90	17	225	1
					226	2
					227	3
					228	4
			180	18	242	1
					230	2
					231	3
					233	4
B7	9.4	BNi-3	30	10	364	1
					365	2
					366	3
					367	4
			90	11	368	1
					369	2
					370	3
					371	4
			180	12	372	1
					373	2
					374	3
					375	4
B8	9.4	BNi-2	30	22	252	1
					253	2
					254	3
					255	4
			90	23	256	1
					257	2
					258	3
					259	4
			180	24	260	1
					261	2
					262	3
					263	4

Table 3. Bacterial Strains Used to Inoculate the Bioreactors

Micro-Organisms
Sphingomonas paucimobilis
Variovorax paradoxus
Acidovorax delafieldii
Stenotrophomonas maltophilia
Hydrogenophaga pseudoflava
Pseudomonas stutzeri
Comamonas acidovorans
Unidentified Gram negative rod (Rhizobium)

mixture of sterile, filtered (in-line vent filter, 0.2 μ) compressed CO_2 and oxygen (O_2) gas (50:50) into the IATCS solutions. [4] A control program (Labview™) was used to monitor and adjust the pH of the IATCS solutions via measurement of time-course grab samples—once per week. When the pH increased above 8.3 by the pre-set tolerance of ≥0.05 units, solenoid valves opened to allow CO_2/O_2 gas flow into the bioreactor IATCS solutions via glass dispersion tubes (sparging stones). The pH values of the IATCS solutions were recorded weekly over the duration of the test (180 d).

Temperature Monitoring and Control - The MAT system bioreactors and flow cells were housed in microbiological incubator cabinets set at 27±1 °C. The MAT system automatically measured the temperature of the IATCS solutions and the room temperature in which the test was conducted every 10 min throughout the 180-d exposure period.

Microbial Growth Monitoring and Control - The number of inoculated bacteria in the bioreactor IATCS solutions was monitored once a week using viable culture methods. [5] Aerobic heterotrophic medium (R2A) was used to determine the viable count of the bioreactors. Reinoculation of the MAT bioreactors was performed as needed, based upon maintaining a titer of ≥1×10⁵ CFUs/mL.

Total Organic and Inorganic Carbon Monitoring - Forty milliliters of IATCS solution was collected biweekly from each bioreactor into Environmental Protection Agency- (EPA-) approved, organic-free bottles (level 1, amber environmental sample vials, Eagle Picher, Miami, OK) and analyzed for TOC and TIC levels (EPA method 415.1).

Dissolved Oxygen Monitoring - Five milliliters of IATCS solution were collected biweekly from each bioreactor into 25-mL beakers and analyzed for dissolved oxygen (DO) levels using a DO probe (Extech, Model 407510, Waltham, MA).

BIOLOGICAL ANALYSES OF COUPONS - Coupons were evaluated for corrosion and biofilm formation at 30,

90, and 180 d of exposure to the IATCS solutions. Flow cells for each time point were removed from the MAT system and the sample backing plates removed. Coupons were removed using a sterile scalpel to cut the silicone adhesive along the edge of each coupon. The second coupon downstream of the flow cell inlet was evaluated for biofilm using viable culture and scanning electron microscopy (SEM) techniques. [6] The other three replicate coupons were analyzed for corrosion damage.

Biofilm Coupon Swab Viable Culture - A sterile, cotton-tipped swab was used to sample a defined surface area of the biofilm test coupons for viable count determination. A sterile stainless steel plate with a 1-cm-diameter hole was used as a template for collecting a surface sample using the swab. The area sampled on the coupon—determined by the template hole—was swabbed and the swab placed into 5 mL of sterile IATCS solution of the appropriate pH and 3-mm glass beads to aid in dispersion. The biofilm swab sample was sonicated in an ice-cold water bath three times for 10 s each. The sample tube was then vortexed at high speed for 60 s. The dispersed sample was serially diluted into IATCS solution and 0.1 mL of each dilution spread-plated in duplicate onto R2A agar. Additionally, 3 mL of the swab dispersion buffer was membrane filtered (Nalgene® filter funnel, 0.45-μ gridded cellulose nitrate) and the membranes plated onto R2A. R2A plates were incubated aerobically at 30 °C for 7 d, then enumerated for CFUs.

Analysis of Sulfate-Reducing Bacteria - One milliliter of the swab dispersion buffer was inoculated into Butlin's medium vials for detection of SRB. [7] The Butlin's medium vial contained a seal with a butyl rubber septum for inoculation of IATCS fluid samples via syringes and a mild steel nail for detection of hydrogen sulfide generation. The inoculated media vials were then incubated at 30 °C for 14 d. Formation of a black precipitate on the nail and in the bottom of the vial indicated growth of SRB.

Biofilm Coupon SEM - Samples for biofilm analysis using SEM were removed from test coupons by cutting an approximately 0.25-in by 0.25-in sample section from the overall coupon using IPA-cleaned sheet metal snips. The sample section was removed from the upper-right corner of the coupon for all SEM biofilm evaluations at each test time point. Coupon sample sections were placed in 2 mL of sterile, filtered (0.45-μ cellulose acetate membrane) fixing solution containing 3% (v/v) glutaraldehyde in 0.1 M sodium (Na) cacodylate solution for at least 5 min. Coupons were then fixed in 2 mL of sterile, filtered 1% (v/v) osmium tetroxide in 0.1 M Na cacodylate solution for 2 min. After fixing, the coupons were washed in sterile, filtered 0.1 M Na cacodylate solution three times for 2 min, then rinsed with dilute 1:1 (v/v) 0.1 M Na cacodylate solution. Coupons were then

dehydrated by immersing for 2 min in a series of increasing concentration of ethanol washes beginning with 40% and increasing to 80% in 10% (v/v) increments. The ethanol washing series was then increased in concentration by 5% increments to 100% and coupons stored in the 100% ethanol at 5 °C prior to critical point drying. [8]

Dehydrated coupons were critical point dried (CPD) in liquid CO_2 using a critical point dryer (Smdri PVT-3B, Tousimis Research Co., Rockville, MD). After CPD, coupons were sputter coated with gold using an SPI-Module Controller and Sputter Coater (Structure Probe, Inc., Westchester, PA). The unit is equipped with a pure gold anode for sputtering. Coupons were pumped down to approximately 5×10^{-1} mbar and purged with a small amount of inert argon gas during coating. Coupons were then sputtered up to four times for 40 s each run, depending on the coating thickness desired (determined by SEM). Gold-coated coupons were analyzed for presence of biofilm and photographed using a Cambridge Stereoscan Model S-240 scanning electron microscope (Leo Electron Optics, NY).

CORROSION ANALYSES - At each end point (30, 90, 180 d), eight flow cells were removed from the MAT system and the samples examined for damage. After removal of the corrosion samples, they underwent the following processing and analysis to quantify the corrosion damage:

- Cleaning with isopropanol to remove the biofilm.
- Digital imaging (macrophotographs).
- SEM examination of the sample surfaces.
- Sectioning, mounting, and metallographically polishing the resulting cross sections.
- Sputter coating the mounts with gold and examination by SEM.
- Repolishing the mounts, then etching and examination by optical microscopy.

This listing is chronological. For comparative purposes, new, unexposed samples underwent the same processing and analysis.

Exposure Macrophotographs - Prior to initiation of the test, digital images of the samples mounted to the flow cells were taken to compare to the samples after testing. Posttesting images were taken after the samples were removed from the flow cell and were cleaned with isopropanol. After removal from the flow cell, samples were stored in a desiccator when not being analyzed.

Sample Surfaces - SEM images of the samples' surfaces were acquired in three regions. In the braze and Ni strip regions, samples were scanned at low magnification until the area showing the observed worst-case damage was located. At this location images were acquired at magnifications of × 50, × 500, × 1000, × 5000, and × 10,000. All SEM magnifications are approximate. Since the fillet area showed a great deal of morphological variation, only a × 50 image was obtained.

Sample Sectioning and Mounting - From each flow cell, the second sample from the outlet—position No. 3—of the flow cell was sectioned. The sectioning line passed through the cut corner and Ni strip of the sample to allow for subsequent analysis of these regions. The larger remnant and all other uncut samples were stored in a desiccator for possible future analysis. The smaller piece resulting from the cut was cold mounted in epoxy and metallographically polished.

SEM of Cross-Sectioned Samples - As the mounting material was nonconductive, the cross-sectional mounts were sputter coated with gold to allow for examination by the SEM. Imaging of the three regions was carried out at magnifications of × 5000 and × 10,000. One location on the fillet and Ni strip and three locations on the brazing were examined. Additionally, one location at the cut corner edge was documented. For all regions, the perceived worst-case locations were documented. The magnifications used did not allow for thickness measurements to be made from these images; therefore, the focus of this examination was to locate surface areas exhibiting possible damage.

Optical Microscopy of Cross Sections - Atomic force microscopy showed that the brazing is not flat. The topography of the samples makes it difficult to locate small areas of attack and to establish a baseline from which to measure depths. For example, if material loss adjacent to the area of attack has occurred, the material loss measurement will be artificially low. Therefore, for the braze region of the samples, optical microscopy of metallographically prepared cross sections was used to determine a sample's average minimum and maximum thickness and associated standard deviation. For these braze thickness measurements, the braze to base metal interface was chosen to provide a reference point that was unaffected by exposure. The disadvantage of this technique is that inherent surface roughness and variations in brazing thickness will determine the detection limits of the material loss measurements. The inherent roughness of the samples is illustrated by the circled areas of the unexposed samples shown in figures 1 and 2. Additionally, these figures show that localized areas of the unexposed samples exhibit a similar morphology, as may be expected if localized attack was to have occurred.

After the mounted cross-section samples were examined with the SEM, the samples were repolished to remove the gold plating and etched to reveal the braze to base metal interface. A magnification was chosen, such that both the brazing outer surface and brazing/base metal interface could be imaged, allowing for brazing thickness measurements. One location at the cut corner edge, fillet

Figure 1. Optical Microscopic Image of the Braze of Sample 204

Figure 2. Optical Microscopic Image of the Braze of Sample 308

and Ni regions, and four locations approximately equally spaced in the braze region were photodocumented. Additionally, the brazing was scanned to photodocument the observed worst-case/thinnest location. Braze thickness was measured with an imaging and measurement software program. Measurement of a fixed 0.01-mm (0.3937-mil) distance on a stage micrometer indicated that measurements were reproducible to ±0.0039 mil. Additionally, the average of 10 measurements equaled the calibrated distance of 0.01 mm. All measurements were made in millimeters, to the ten-thousandths digit, and were subsequently converted to thousandths of an inch (mil).

CHARACTERIZATION OF UNEXPOSED SAMPLES - The methodology used to analyze the unexposed and exposed samples is similar. Slight modifications to the optical microscopy of the cross-sectioned samples methodology were made. These differences were as follows: (1) The unexposed samples were sectioned three times, and all three sections were mounted and the braze thickness quantified as described previously in the Optical Microscopy of Cross Sections section, and (2) two BNi-2 and two BNi-3 samples were examined at a total of 12 randomly spaced locations and five observed minimum values were documented per sample type. For each sample type, one sample was sectioned normal to the Ni strip and the other parallel to the strip. This allowed for the investigation of any anisotropic behavior of the braze thickness, and the determination of any braze thickness variation in the vicinity of the fillet.

UNDER BIOFILM CORROSION EVALUATION - BNi-2 sample 215 was chosen for evaluation of corrosion damage associated with biofilm features. This sample was chosen because one of the microcolonies found on its surface was distributed over an area of ≈1 mm². This allowed the mapping of its location on the coupon at lower SEM magnification before and after removal of the biofilm. Most microcolonies that were found on the other test coupon samples were smaller, making them difficult to locate after cleaning. After the microcolony's location had been mapped, the biofilm on the coupon was
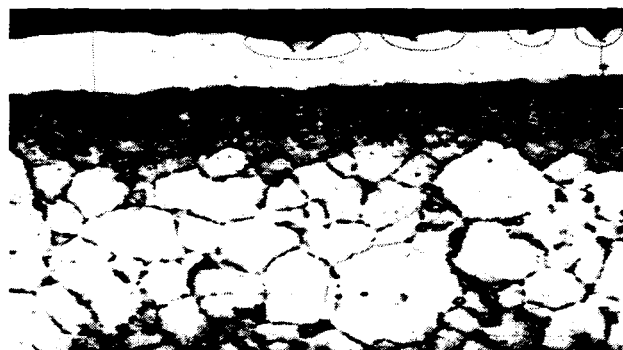
removed by immersing the coupon in an ultrasonic acetone bath for 30 s, and then examined with a SEM for indications of damage.

RESULTS

TEST MONITORING AND CONTROL

Flow Rate - A flow rate of 0.33 ft/s was maintained for the duration of the test.

pH Monitoring and Control - The IATCS solutions were maintained at pH 8.3 or 9.4±0.2 throughout the 180-d exposure test period. The pH of the 9.4 IATCS bioreactors equilibrate to the reported 9.2 pKa of the borate buffering system in the solution after 60 d. Maintenance of the 8.3 pH IATCS bioreactors at the desired tolerance required that they be sparged with the CO_2/O_2 gas mixture at a flow rate of 85 scc/m for 1 min approximately twice per week.

Temperature Monitoring and Control - The data show that the bioreactors were maintained at a temperature of 27±1 °C throughout the 180-d exposure test period.

Total Organic and Inorganic Carbon Monitoring - The pH 8.3 bioreactors (A1, A2, B5, and B6) had significantly higher TIC levels than the 9.4 pH bioreactors (A3, A4, B7, and B8). This is attributed to the controlling of the pH 8.3 bioreactors using the CO_2 gas mixture. Bioreactor B5 showed consistently higher TIC levels than the other pH 8.3 bioreactors. The pH 9.4 bioreactors showed a trend of increasing TIC levels throughout the exposure test period and achieved levels of ≈25 mg/L by the test end.

At the start of the test, the TOC in the bioreactors ranged from 35 to 98 mg/L. After 2 wk of operation, the bioreactor TOC levels dropped an average of 26 mg/L.

Dissolved Oxygen Monitoring - The MAT bioreactor total DO levels increased over the course of the exposure test.

Microbial Growth Monitoring and Control - The test bioreactors were inoculated with the bacterial consortia at the required concentration of 1×10^6 CFUs/mL. After 2 wk of operation, the MAT bioreactors A3 and A4 dropped below the required viable count level of 1×10^6 CFUs/mL and were reinoculated with the test strains. All of the inoculated bioreactors dropped ≈1 log in growth level after 60 d of operation and maintained levels of approximately 1×10^5 CFUs/mL to the end of the exposure test period. The bioreactors were maintained at the 1×10^5 CFUs/mL level and were not reinoculated with the test species.

Control bioreactor B6 showed growth of bacteria after 40 d of operation. Control bioreactors B5, B7, and B8 showed no signs of growth throughout the 180-d test period.

Sulfate-Reducing Bacteria - The SRB *D. desulfuricans* (ATCC 7757) was inoculated into the test bioreactors A1–A4 at the start of the exposure testing. The organism was only recovered from the MAT IATCS fluid of bioreactor A2, 1 wk after it was inoculated. The organism was not recovered from any of the inoculated bioreactors' IATCS fluid or from surface swabs of the biofilm coupons at the 30-d exposure time point.

Sterile, filtered sodium sulfate (Sigma Chemical, product S6547) solution was added to all of the MAT bioreactors to a final concentration of ≈1.8 ppm at day 40 of the exposure test.

The SRB was reinoculated into bioreactors A1–A4 at day 50 of the exposure test. The organism was not recovered from any of the inoculated bioreactors' IATCS fluid or from surface swabs of the biofilm coupons at either the 90- or 180-d exposure time points.

BIOLOGICAL ANALYSIS OF COUPONS

Biofilm Coupon Swab Viable Culture - Figure 3 illustrates the MAT biofilm coupon viable counts at 30-, 90-, and 180-d exposure testing. The data indicate that the coupon materials were colonized at increasing levels over time. Although no attached bacteria were found on the surface of control coupons in bioreactor B6, the bacterial concentration in the fluid of that bioreactor remained constant after it became contaminated.

Except for the 30-d biofilm viable count from the coupon of bioreactor A1, there was no significant difference in colonization levels between the different ISS heat exchanger materials under the different test conditions at each time point. The significantly higher viable count from the 30-d bioreactor A1 coupon sample could be attributed to sampling error associated with the presence of biofilm slime—evident in the flow cell, and sample evidence of yellow slime formation on interior surfaces at all time points.
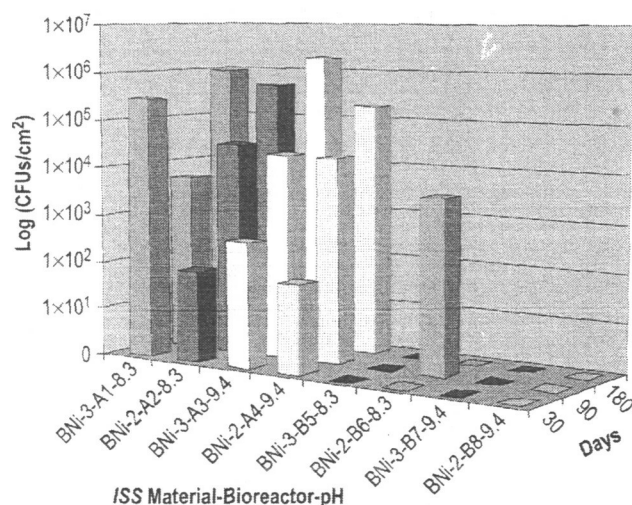

Figure 3. Colonization of *ISS* Heat Exchanger Materials

Biofilm Coupon SEM - SEM analysis of the 30-, 90-, and 180-d biofilm coupons showed that the *ISS* test material surfaces were colonized by the test isolates in the form of biofilms composed of single cells and heterogeneous, localized microcolonies that ranged from 5 μ to 1 mm^2. There was no apparent difference between the braze material and Ni strip of the *ISS* materials for colonization characteristics. There was also no apparent difference between the test conditions for colonization characteristics of the inoculated test materials.

Except for the 90-d exposure coupon from bioreactor B6, control uninoculated coupons showed no evidence of colonization over the course of the exposure test. The 90-d exposure coupon from bioreactor B6 showed evidence of colonization; however, the 180-d exposure coupon from B6 showed no evidence of single cells or microcolonies. This was consistent with the lack of recovery of viable bacteria from the swab sample taken from the coupon. The bulk IATCS fluid from B6 at the 180-d time point indicated that the contaminating bacteria were at the expected viable count level.

CORROSION DAMAGE ANALYSES

Characterization of Unexposed Samples - Unexposed/ baseline samples were characterized using the same techniques as the end point samples, except as noted in the Characterization of Unexposed Samples section. The maximum and minimum brazing thickness, as determined by optical microscopy of cross-sectioned unexposed samples, are shown as the shaded regions of figures 4–11. No anisotropic behavior of the braze thickness was observed, but thickening of the braze in the vicinity of the fillet was observed. For this reason, locations close to the fillet region of the end point and unexposed samples were not analyzed.
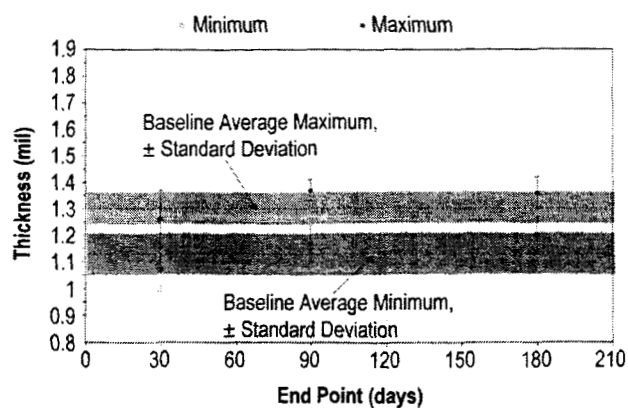
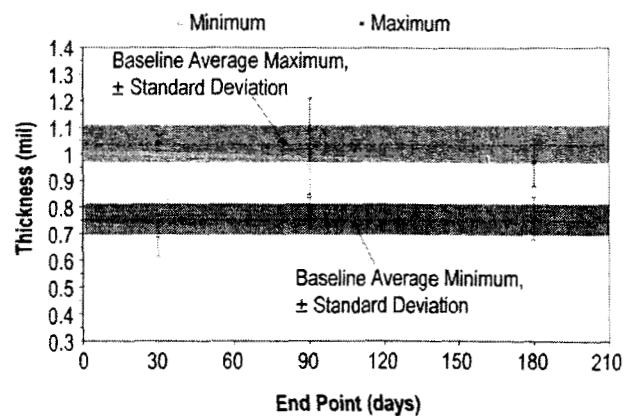**Figure 4. Brazing Thickness Values for BNi-2 Samples Exposed to pH 8.3 and Inoculated Conditions**

Figure 5. Brazing Thickness Values for BNi-3 Samples Exposed to pH 8.3 and Inoculated Conditions
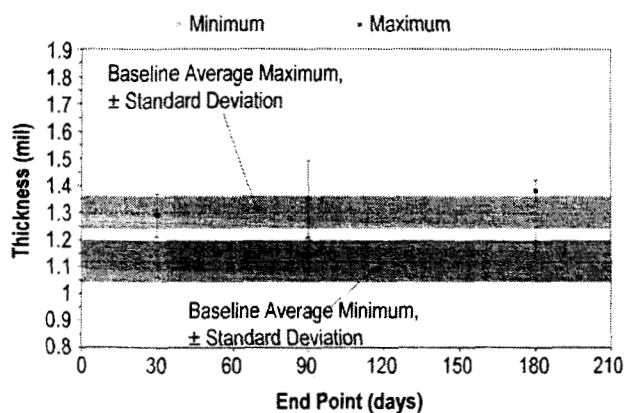

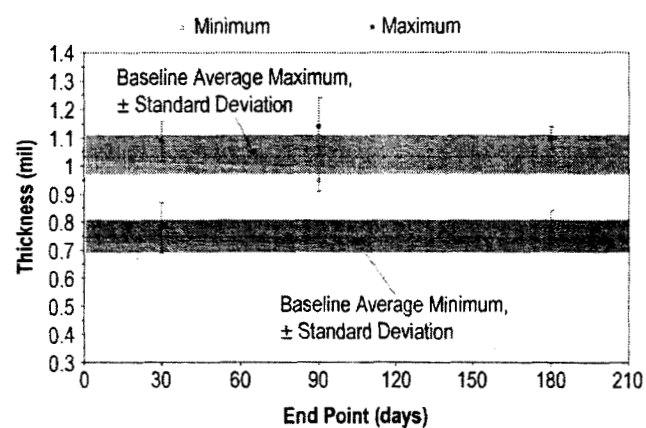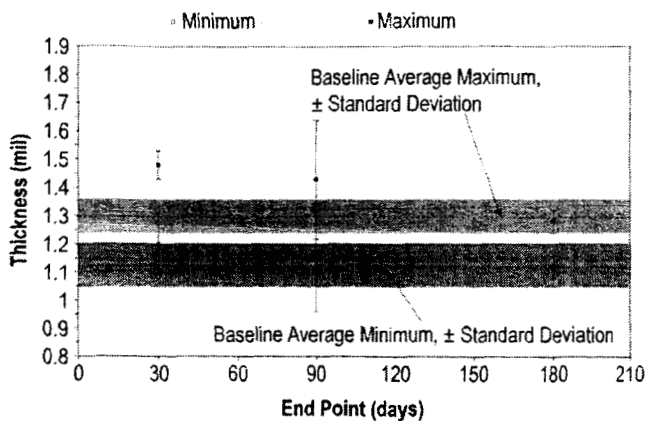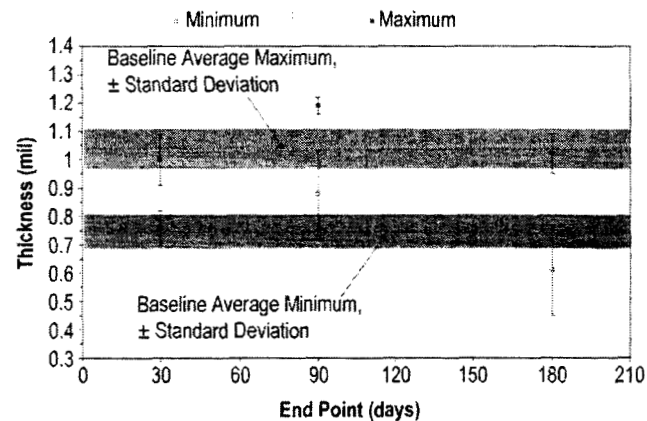**Figure 6. Brazing Thickness Values for BNi-2 Samples Exposed to pH 8.3 and Uninoculated Conditions**

Figure 7. Brazing Thickness Values for BNi-3 Samples Exposed to pH 8.3 and Uninoculated Conditions

Figure 8. Brazing Thickness Values for BNi-2 Samples Exposed to pH 9.4 and Inoculated Conditions

Figure 9. Brazing Thickness Values for BNi-3 Samples Exposed to pH 9.4 and Inoculated Conditions

Figure 10. Brazing Thickness Values for BNi-2 Samples Exposed to pH 9.4 and Uninoculated Conditions
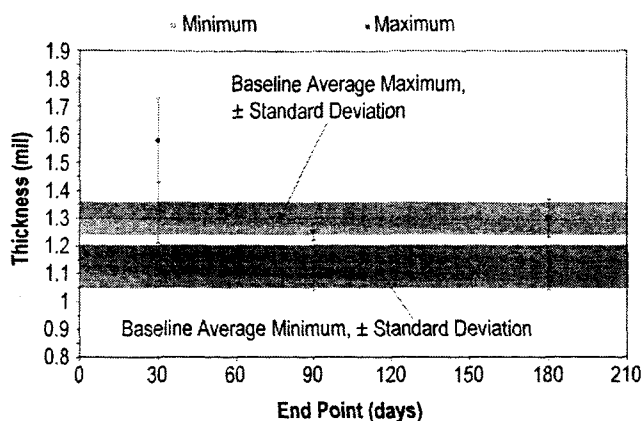

Figure 11. Brazing Thickness Values for BNi-3 Samples Exposed to pH 9.4 and Uninoculated Conditions

A number of interesting trends concerning the unexposed samples were found in this study. The BNi-2's unexposed average minimum thickness (1.13 mil) is greater than BNi-3's average unexposed maximum thickness (1.04 mil); i.e., the BNi-2 braze is initially thicker. The increased distance between the maximum and minimum average thickness values of the BNi-3 samples indicates that these samples are initially rougher than the BNi-2 samples.

Exposure Macrophotographs - The 30-d BNi-2 and BNi-3 samples did not show any discernable differences relative to the unexposed samples after exposure. Some of the 90-d samples (324, 326, 327, 338, 356, and 358) did show some darkening postexposure. Orange staining and/or significant darkening of some of the 180-d samples (328, 330, 331, 340, 350, 351, 360, and 372) were noted. It is interesting to note that all of these samples are of the BNi-3 type. It was observed that the samples would darken with exposure to light.

SEM of Sample Surfaces - Needle-like features were found on the BNi-2 samples. Energy-dispersive spectrometry (EDS) of these features showed them to be chromium rich. Similar features were not observed on the BNi-3 samples. Unexposed and exposed samples also showed pores at grain boundary triple points and a dark phase, especially in the vicinity of the fillet, between grains. At higher magnifications, 180-d samples 250, 231, and 262 may show some indications of attack at the braze grain boundaries. However, as shown in the following sections, these features were too minor to be quantified by the other analytical techniques employed in this study. Additionally, EDS spectra did not indicate the presence of corrosion products, and the baseline samples that were not exposed showed similar features. As such, it is not possible to conclude that the observed features are indeed corrosion damage. If these features are the result of localized corrosion, longer exposure times would result in better resolution and perhaps measurable corrosion damage. If a feature of interest
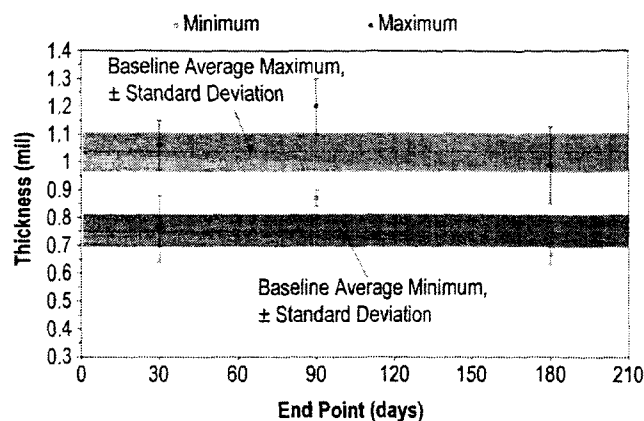
was observed, EDS was performed to determine if a corrosion product was present.

SEM of Cross-Sectioned Samples - Both the BNi-2 and BNi-3 samples did not show any significant differences relative to the unexposed samples. If a feature of interest was observed, EDS was performed to determine if a corrosion product was present. These EDS spectra did not indicate the presence of corrosion products.

Optical Microscopy of Cross-Sectioned Samples - Figures 4–11 show the average minimum and maximum braze thickness values and associated standard deviation for the approximately evenly spaced locations of the unexposed and end point samples. To facilitate comparison, each sample type is plotted on identical y axes, and the thickness is plotted over the same range (1.1 mil) independent of sample type. The averages for the end point samples are represented by either a hollow square (minimum) or a filled square (maximum) and the standard deviation by error bars. The average minimum and maximum thickness of the unexposed samples are represented by horizontal dashed lines. Additionally, a shaded region, with a height of plus/minus the standard deviation of the associated averages, is centered on the baseline average values. The error bars and shaded regions then provide a measure of the scatter associated with the minimum and maximum values, and the distance between the maximum and minimum a measure of the samples' roughness. Graphing both the unexposed and end point data in this manner allows for comparison of the unexposed and end point samples and of inoculated versus uninoculated effects.

Fillet Region - The fillet regions of the end point samples did not show any discernable differences relative to the unexposed samples. The etchant used for the optical braze thickness measurements appeared to have preferentially attacked the fillet regions, making analysis difficult. Additionally, these areas were not uniform.

Under Biofilm Corrosion Evaluation - Figure 12 illustrates the results of biofilm removal from the surface of BNi-2 sample 215 for examination of the condition of the underlying brazing. The position of the targeted microcolony on the coupon was mapped using SEM at low magnification. Vein-like features extending out from the fillet of the sample served as landmarks for locating the microcolony after cleaning of the coupon. The result of the cleaning was that the microcolony was removed, along with its gold coating, leaving a footprint of the area it had once covered. The footprint resulted from the contrast between the areas underneath the microcolony that were exposed (dark color) from cleaning and the areas outside of the microcolony that remained coated with gold after cleaning (light color).

Figure 12(e) shows the characteristics of the microcolony. The microcolony was heterogeneous in its distribution and thickness of microbial cells. Likewise, figure 12(f) shows the area depicted in figure 12(e) with approximately $\times 4$ less magnification after cleaning. The contrast between the gold-coated areas and the areas cleaned of biofilm are apparent. The brazing of the coupon underneath where the microcolony was removed showed no damage. Figures 12(g) and 12(h) show the areas depicted by the arrow and square, respectively, in figure 12(f). These figures do not show evidence of corrosion attack of the brazing grains or grain boundaries underneath the microcolony. Additionally, no attack in the immediate vicinity of the microcolony was observed.

DISCUSSION

CORROSION DAMAGE EVALUATION - The end point braze thickness data were analyzed graphically and statistically.

Graphical Analysis - In this analysis of the braze thickness data, a significant difference was said to exist when an end point sample's maximum or minimum value did not graphically fall within the corresponding maximum or minimum shaded region of the unexposed samples. The end point sample was defined as the entire range represented by the error bars. As none of the samples showed the formation of corrosion products on their surfaces, end point samples whose thickness values were above the corresponding shaded region were considered not to have experienced corrosion-related damage. However, samples whose end point values fell below their corresponding unexposed shaded region were considered to be candidates that may have experienced corrosion-related damage. Reviewing figures 4–11 with this criterion in mind, none of the samples showed corrosion-related damage. There are two 180-d samples whose minimum values almost do not meet this criterion; namely, samples 362—exposed to pH 9.4 and inoculated conditions, and 374—exposed to pH 9.4 and uninoculated conditions. However, the

(a)　　　　　　　(b)

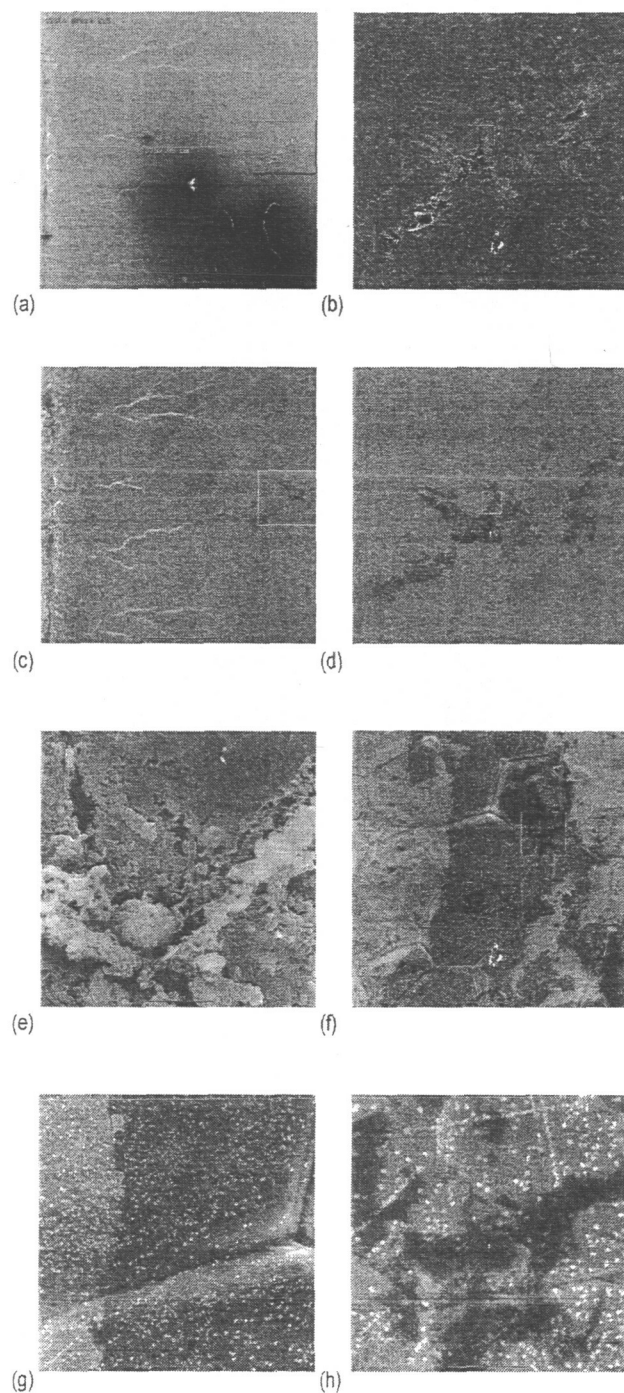(c)　　　　　　　(d)

(e)　　　　　　　(f)

(g)　　　　　　　(h)

Figure 12. Under Biofilm Corrosion Evaluation of BNi-2 Sample 215 From Bioreactor A2, Flow Cell 15 (180-d Exposure): (a) Location of Biofilm on Test Coupon; (b) Magnification of Area Depicted by Square in Photomicrograph (a); (c) Location of Biofilm Area After Cleaning of Coupon for Under Deposit Analysis; (d) Magnification of Area Depicted by Square in Photomicrograph (c); (e) Magnification of Area Depicted by Square in Figure 1, Photomicrograph (b); (f) Magnification of Area Depicted by Square in Figure 1, Photomicrograph (d); (g) Magnification of Area Depicted by Arrow in Photomicrograph (f); and (h) Magnification of Area Depicted by Square in Photomicrograph (f).

other analyses performed on these samples did not show any indication of corrosion damage.

As shown above, the criteria used in the graphical analysis sets the detection limit for corrosion-related damage. Consider sample 374 for example. For the BNi-3 samples, the standard deviation of the minimum thickness of the unexposed samples was 0.06 mil and the standard deviation of sample 374's minimum thickness was 0.04 mil. Therefore, for this sample, the detection limit was 0.1 mil.

Statistical Analysis - As the baseline samples are not smooth and the braze thickness is not uniform from sample to sample, statistics were used as a second technique to help determine if a significant difference between the baseline and exposed samples existed. The student's t-test was used to determine if there was a statistically significant difference between the average minimum thickness measured at time zero (unexposed) and after the different exposure times. Significance tests were performed to determine if the average minimum brazing thickness for each exposure condition was different than the initial baseline average minimum thickness. The tests were carried out at the 95% confidence limits. [9,10]

SUMMARY AND CONCLUSIONS

The MAT system successfully simulated the *ISS* IATCS heat exchanger environment. It maintained the test coupons exposed to environmental conditions identified as critical/optimal for biofilm formation and MIC, but within the operational parameters of the *ISS* hardware. The parameters included pH, temperature, flow rate, available nutrients, and microbial concentrations. Microgravity conditions were not duplicated due to the difficulties of establishing such conditions on Earth. Microgravity was not considered a critical parameter needed to achieve the test objectives.

Analysis showed that under the test conditions, localized biofilm started to form on both types of coupons tested— BNi-2 and BNi-3—within the first month of test. SEM images showed that the surfaces were colonized by a combination of single cells and heterogeneous localized microcolonies that ranged from 5 μm^2 to 1 mm^2 after 6 mo of exposure. There was no significant difference in the microbial colonization on the surface of the two different test materials under the two test conditions—pH 8.3 and 9.4±0.2.

All the control bioreactors, except B6, maintained abiotic conditions and provided a baseline of the environmental effects to the materials, independent from microorganisms. This was important information that was used for data interpretation.

In an attempt to expose the coupons to bacteria known to initiate/accelerate corrosion, the test bioreactors were inoculated with the SRB *D. desulfuricans*. The bacterium was expected to survive and colonized the material if conditions were favorable for its survival. Test data showed that *D. desulfuricans* survived for a few days but were not recovered from the system after test completion.

Direct examination of the surface underneath and in the vicinity of an ≈1-mm^2 microbial colony on a BNi-2 coupon sample showed no evidence of corrosion associated with this microbial colony. There was no indication that the formed biofilm in that area affected the surface of the material after 6 mo of exposure. This was only one data point (one microcolony) and analyses of additional microcolonies are needed to verify this finding.

Analyses of the MAT corrosion data showed that topography changes resulting from corrosion during the exposure time were similar to preexisting surface imperfections. Significant/detectable differences between the unexposed 30-, 90-, and 180-d end point samples and the test coupons were not found.

No significant corrosion damage, and specifically no MIC, was identified in this study. In an effort to understand if MIC/corrosion is or will be an issue in the *ISS* IATCS, it is recommended that the exposure period be increased in future testing. The analyses of IATCS flight hardware will ultimately help validate the results of this test.

ACKNOWLEDGMENTS

REFERENCES

1. Hurst, C.J. (ed): *Manual of Environmental Microbiology,* 2nd ed., pp. 1072–1083, ASM Press, Washington, DC, 2002.
2. Kearns, J.R.; and Little, B.J. (eds): *Microbiologically Influenced Corrosion Testing,* pp. 1–293, ASTM Publication, Philadelphia, PA, 1994.

3. Atlas, R.M.: *Handbook of Microbiological Media*, 2nd ed., CRC Press, NY, 1997.

4. "IATCS Fluid pH Adjustment With CO_2," Hamilton Sundstrand Internal Memo, November 2002.

5. *Standard Methods for the Examination of Water and Wastewater*, 19th ed., pp. 9-31–9-38, APHA, AWWA, WEF, Washington, DC, 1995.

6. Mittelman, M.W.: *Laboratory Studies of Bacterial Biofilms in: Techniques in Microbial Ecology*, R.S. Burlage, R. Atlas, D. Stahl, G. Geesey, and S. Sayler (eds.), pp. 337–353, Oxford University Press, Inc., New York, NY, 1998.

7. Mittelman, M.W.; and Geesey, G.G.: *Biological Fouling of Industrial Waters: A Problem Solving Approach*, Micro Water Associates, San Diego, CA, 1987.

8. Gu, J.; Ford, T.E.; and Mitchell, R.: Susceptibility of Electronic Insulating Polyimides to Microbial Degradation, *J. Appl. Polymer Sci.*, Vol. 62, pp. 1029–1034, 1996.

9. Walpole, R.E.; and Myers, R.H.: *Probability and Statistics for Engineers and Scientists*, MacMillion Publishers, New York, NY, 1978.

10. Spiegel, M.R.: *Statistics, Schaum's Outline Series*, McGraw-Hill, New York, NY, 1961.

ACRONYMS AND SYMBOLS

Ag	silver
Ag_2SO_4	silver sulfate
BNi	braze material with nickel filler
CFU	colony-forming unit
CO_2	carbon dioxide
CPD	critical point dried
DO	dissolved oxygen
EDS	energy-dispersive spectrometry
EPA	Environmental Protection Agency
IATCS	Internal Active Thermal Control System
IPA	isopropyl alcohol
ISS	*International Space Station*
LTL	low-temperature loop
MAT	microbiologically influenced corrosion accelerated test
MIC	microbiologically influenced corrosion
MTL	moderate-temperature loop
Na	sodium
Ni	nickel
$NiPO_4$	nickel phosphate
O_2	oxygen
PO_4	phosphate
SEM	scanning electron microscopy/microscope
SRB	sulfate-reducing bacteria
TIC	total inorganic carbon
TOC	total organic carbon